The United Nations University

GEOTHERMAL TRAINING PROGRAMME
Orkustofnun, Grensásvegur 9,
IS-108 Reykjavík, Iceland

Reports 1996
Number 14

MONITORING OF PRODUCTION DECLINE AND PRESSURE DRAWDOWN IN GEOTHERMAL RESERVOIRS USING DECLINE CURVES ANALYSIS METHOD

Rosanna A. Requejo
Geothermal Division, Energy Resource Development Bureau,
Department of Energy,
PNPC Complex, Merritt Road,
Fort Bonifacio, Metro Manila,
PHILIPPINES

ABSTRACT

The application of the decline curves analysis method on the monitoring of production decline and pressure drawdown in geothermal reservoirs was studied. Two geothermal production fields were selected, the Bacon-Manito I in the Philippines and Krafla in Iceland. It was not possible to pursue the analysis for Bac-Man I at this point in time, primarily because there was no substantial and crucial pressure drawdown manifested in the pressure profiles of the five chosen production wells of the field. However, conclusions were drawn that proper resource management is being implemented in the field by the developer and that currently there are no signs of over-exploitation of the resource. In Krafla, it was concluded that the nonlinear second order exponential decay function predominantly defines the trend in production decline observed in Krafla field, based on the result of comparison between the average values of χ^2 (Chi-Square) obtained from the exponential decay and linear (harmonic) functions. With the simulator program HOLA and the assumed depletion trend in the reservoir pressure of well KJ-18, it was established that KJ-18 pressure drawdown can explain the observed production decline in wells KJ-14, KJ-17 and KJ-19. Estimates of future descent in production of these wells can, therefore, be predicted, assuming KJ-18 pressure depletion trend and with the employment of the second order exponential decay function. In conclusion, the decline curves analysis method can be one efficient tool for the DOE in the performance of its monitoring and regulating function. The technique can enable the Department of Energy (DOE) in the Philippines to analyze the trend in the reservoir pressure depletion and production decline of different geothermal production fields in the country, and to estimate future declining trends. Hence, it can state whether proper resource management strategies are being applied a the field, or whether over-exploitation of the resource is to be expected.

1. INTRODUCTION

The Department of Energy (DOE) in the Philippines is a government institution fundamentally mandated among others to establish and administer programmes for the exploration, transportation, marketing and storage of energy resources of all forms, and to regulate and exercise full supervision and control over all government and private energy-related projects and activities to ensure proper exploitation, utilization and management of the country's indigenous resources.

Under the DOE are four skeletal bureaus, a part of one of them being the Geothermal Division. This division is mandated, among others, to oversee, monitor and regulate geothermal operations undertaken by both private and government entities to ensure strict compliance to the policies and standards of the State with the end view of nonexploitation and proper management of geothermal resources in the country.

To effectively and competently perform this function, it is of prime importance that ample and competitive knowledge, skills and expertise on the diverse phases and operations of geothermal energy development and utilization be acquired by technical professionals of the Geothermal Division through continuous procurement of specialized training and courses on geothermics being offered by various educational institutions worldwide, including the United Nations University (UNU) in Iceland. With these technical capacities at hand, the division could exercise fully its reputable authority to monitor and regulate all geothermal operations in the country in lieu of its mandate.

The decline curves analysis method was studied as one tool in the monitoring of production and reservoir pressure decline in geothermal reservoirs. A number of literary works on decline curves analysis were reviewed and it was learned that aside from the method's simplicity to utilize, it can also enable estimation of future performance of geothermal reservoirs through extrapolation of future production estimates. This is done simply by fitting the trend of past production performance to either linear (harmonic) or nonlinear functions. The best fit curve is then utilized in the extrapolation procedures.

On the practical application of the decline curves analysis method, two geothermal production fields were studied, namely, Bacon-Manito I in the Philippines and Krafla in Iceland. The computer program Microcal Origin version 4.0 was used in the analysis of the type of fit curves that best define the trend of production descent in these two fields. The relationship with and dependency on pressure drawdown of production decline was also examined and a conclusion was later drawn on how the resulting interconnection between these parameters could be used in the prediction of future production decline employing the obtained best fitting curve function. Finally, a chapter is given on the reservoir parameters to be consistently monitored during exploitation of a geothermal field, and the most compelling parameters signaling the resource's over-exploitation were briefly discussed.

2. LITERATURE REVIEW

In the absence of the effects of scaling, changes in enthalpy and cold water entry on the performance of a particular geothermal well, the decline curves analysis method is a very effective and simple method that can be employed in the monitoring of production and pressure decline in geothermal reservoirs. The method assumes that the mass flow of a well declines smoothly either exponentially or harmonically (i.e. linear) as exploitation reduces reservoir pressures. It predicts future mass flow of a well by treating the past history as a time series, then fitting it to a convenient formula which in turn is used for extrapolation (Grant et al., 1982).

It has been proven that one of the best predictions of future performance of a geothermal reservoir is derived from the decline curves analysis method, even if it is no more than extrapolating a decline of so many percentages per year. However, the technique is limited by the lack of a theoretical basis because it cannot predict the effect of a change in management practice, outside of past variation. The flow of one well can be extrapolated only as long as the control of other interfering wells does not change. For example, if another power plant is added, the trend with time is likely to change (Grant et al., 1982).

But though it has been said that the function of interpolating the history of production does not have a physically precise meaning, it is however useful in the management of the geothermal field for formulating estimates of future production (Neri, 1988).

To have a more tangible understanding of the application of the decline curves analysis method in geothermal reservoirs, a literary research was performed. Two case histories in the Larderello geothermal field in Italy were encountered. In both cases, the decline curves analysis method was employed in defining the best fit curve that characterized the production history of the field, and the relationship of the reservoir pressure history with the field's cumulative production.

2.1 Review on few production decline methods used for geothermal reservoirs

The decline methods developed for analyzing oil and gas wells are used also for geothermal wells but it must be recognized though that petroleum and geothermal reservoirs are very different from each other. Geothermal reservoirs seem to be much more complex than petroleum reservoirs so methods applied in geothermal work must be examined carefully. Still more work must be done as more geothermal fields are produced over time. The following review is based on Zais and Bödvarsson (1980).

2.1.1 Arps method

Arps's work forms the basis for all the decline curve methods currently in use. The most common were graphical in which production q, or cumulative production, is plotted versus time t. Examinations of production data show that data with constant first differences fit an exponential equation, while data with constant second differences fit a hyperbolic or harmonic equation. All three equations can be expressed as

$$a = Kq^{b} = \frac{-dq/dt}{q}$$

where

a = Fractional decline (some authors use D as fractional decline);
q = Production rate of time t;
K = Constant;
b = Constant.

Arps's equations were considered to be strictly empirical until 1973 when Fetkovich proposed some theoretical basis for the exponential equation (Zais and Bödvarsson, 1980). The hyperbolic equation is still considered empirical.

2.1.2 Fetkovich

Fetkovich showed that log-log type curves can be used to analyze production data in an analogous manner to analyze pressure data. He presented log-log plots of dimensionless flowrate vs. dimensionless time

$$q_{Dd} = \frac{q(t)}{q_i} \quad vs. \quad t_{Dd} = D_i t$$

where

D = Decline as a fraction of production rate;
D_i = Initial decline;
q_i = Initial production rate;
t = Time;

for $0 \leq b \leq 1$ and $D_i = 1$.

The solution $b = 0$ is exponential, while $b = 1$ is the harmonic solution. The exponential curve is given by:

$$q_{Dd} = e^{-D_i t}, \quad D_i = 1$$

while the hyperbolic curves are given by

$$q_{Dd} = (1 + bD_i t)^{-\frac{1}{b}} \quad for \ 0 < b \leq 1.$$

Using an overlay technique, production data can be plotted over the curves and a decline exponent can be picked. For $t_{Dd} < 0.3$ all the curves are coincident. Fetkovich showed that the exponential decline has a fundamental base by deriving it as a solution to the constant well pressure case.

2.1.3 Slider's method

Slider proposed a simple method of curve matching to obtain the hyperbolic exponent b and the initial decline rate q_i. To use the method one needs to construct a set of curves of q/q_i vs. log time for various values of a_i and b using Arps's hyperbolic equation. Production data can then be plotted on the curves by using a transparent overlay. The overlay can be moved around until the best fit is found, thus giving b and a_i.

2.1.4 Gentry and McCray

Reservoir analysts have usually assumed that $0 \leq b \leq 1$ in the solution of Arps's equations. There is no mathematical basis for this restriction. Furthermore, $b = 0$ and $b = 1$ are special cases, the exponential and harmonic, respectively, but this does not restrict b from being larger than 1. Gentry and McCray investigated decline curve methods (further description see Zais and Bödvarsson, 1980) using semi-log plots of

$$\frac{q_i}{q} \; vs. \; \frac{Q}{q_i t}$$

Cartesian plots of

$$\frac{q}{q_i} \; vs. \; Q$$

and semi-log plots of

$$\frac{q_i}{q} \; vs. \; a_i t$$

2.1.5 *p/z* vs. *Q*

The natural gas industry has long used decline curves in which pressure divided by gas deviation factor, *p/z*, is plotted against cumulative production, *Q*. The straight line can quite easily be extrapolated to the economic limit of producing pressure. Brigham and Morrow have proposed adapting this method to steam fields. In plotting computer generated data they found that the curve shape was strongly influenced by porosity. Also, the presence of a boiling interface is critical. If the wells are in the vapour zone it would be natural to graph *p/z* versus production, as though this were a gas reservoir, and use an extrapolation of the best straight line as a predictive method to calculate reserves. The efficiency of this technique will be strongly dependent on the porosity if the actual reservoir contains boiling liquid. Further description is given in Zais and Bödvarsson, 1980.

2.1.6 Other decline curve methods

There are two other decline curve methods employed for geothermal reservoirs, namely, Influence Functions, and Linearized Free Surface-Green's Function. For the purpose of this report, these other two methods will not be discussed. The reader is referred to "Analysis of production decline in geothermal reservoirs" by E. Zais and Bödvarsson, 1980 for extensive discussion on the two methods.

2.2 Data analysis

The data can be analyzed by wells, by groups of wells, and by fields. Graphing the data provides an easy way of examining the data for unusual behaviour such as occasional high, low or erratic production. Such data sets can be flagged for special attention. The data can be plotted and analyzed according to Arps using Cartesian semi-log, and log-log plots of production versus time. However, this provides only a "quick look" and further analysis should be done. If the data are smooth enough, then log-log type curves and Gentry's and McCray's curves can be used to fit current data and to extrapolate for future behavior. If the field is vapour-dominated, *p/z* versus *Q* plots can be used but only with great caution.

Production data (*q* versus *t*) can be fitted to Arps's exponential equation using a nonlinear least squares program. The program should calculate R^2 (i.e. correlation coefficient) defined as the regression sum of squares divided by the total sum of squares to indicate goodness of fit. A reasonably high value of R^2, for example greater than 0.65, allows extrapolation with some degree of confidence.

3. THE BACON-MANITO I PRODUCTION FIELD

3.1 Background

The 25,000 hectares Bacon-Manito (Bac-Man) geothermal production field is situated on the boundary of the towns of Bacon in Sorsogon and Manito in Albay provinces on the Bicol Peninsula, Philippines (Figure 1). A first stage geothermal power plant development of 110 MW in the Palayangbayan field sector (Bac-Man I) and a 20 MW_e extension in the Cawayan sector (Bac-Man II) were commissioned in the last quarter of 1993 and first quarter of 1994, respectively. The steam field was developed by the Philippine National Oil Company-Energy Development Corporation (PNOC-EDC) while the power plant was built and operated by the National Power Corporation (NPC); both are government-owned-and-controlled corporations. With this event, Bacon-Manito became the fifth geothermal production field in the Philippines. Ten years had then passed since the last commissioning of two other geothermal power plants in the country.

Exploration work in the Bacon-Manito geothermal field commenced with a reconnaissance survey conducted in 1977 by PNOC-EDC in cooperation with Geothermal Energy New Zealand Ltd. (GENZL) at the Paron, Naghaso, Inang-Maharang and Balasbas areas. The first exploration well, Manito-1 (MAN-1), was spudded on 22 May 1979 and was drilled to a depth of 1,368 m. The well intercepted a downhole temperature of 214°C. The second well, Manito-2 (MAN-2), was spudded on 11 July 1979 with a total

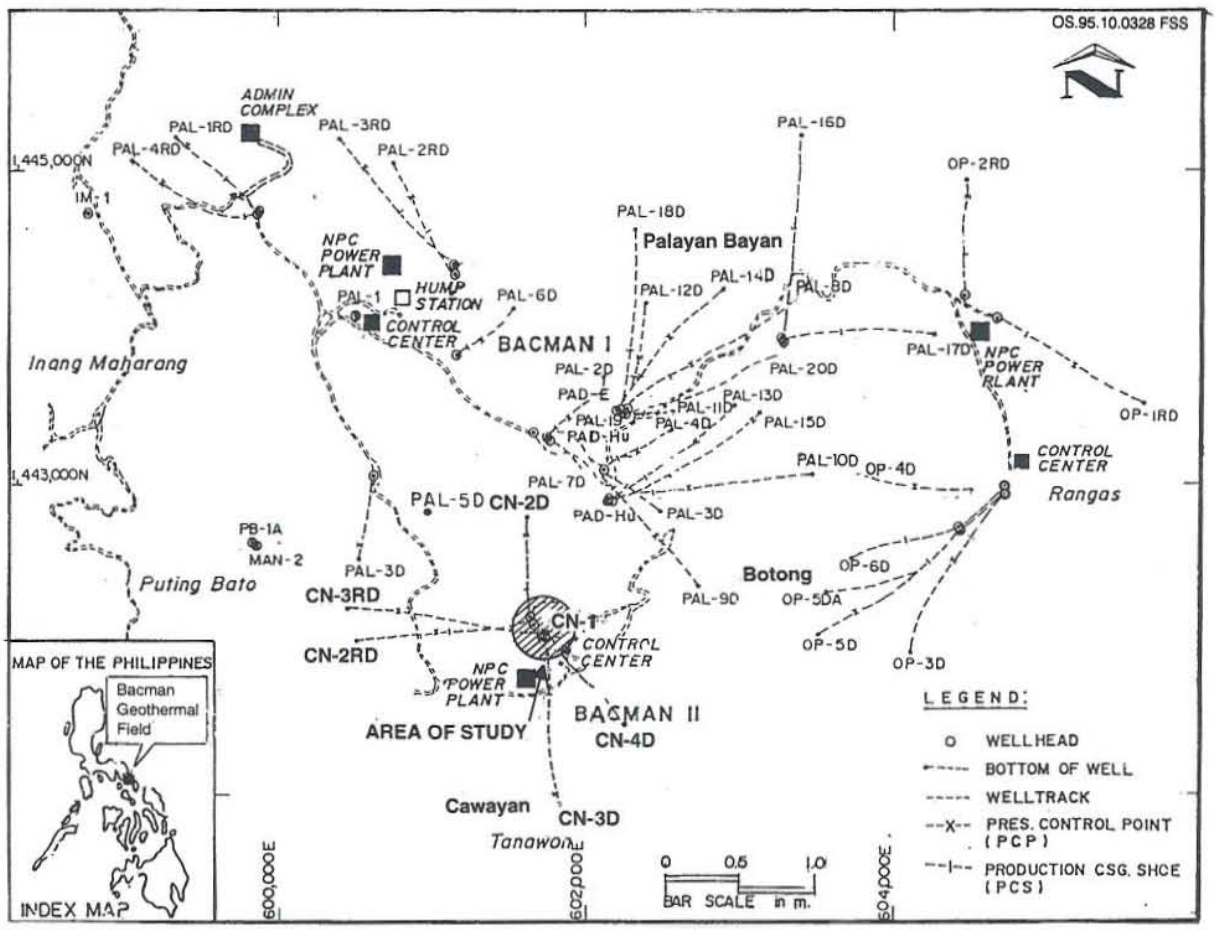

FIGURE 1: The Bac-Man geothermal production field

depth of 1,637 m. Discharge attempts for the two wells using air-compression stimulation and BO-200 boiler, respectively, were unsuccessful. Both wells were, therefore, concluded to be non-commercial. In 1981 the first deep exploratory well, Cawayan-1 (CN-1), was drilled in Cawayan. It was successfully discharged with an initial output of 17.7 MW_e, stabilizing at 11 MW_e and with 0.5% content of non-condensible gases (NCG). With this output, CN-1 became the first commercial well in Bac-Man.

After the production areas were delineated and identified in 1982, extensive production drilling continued in the succeeding years with the first reinjection well drilled at the end of 1988, and the subsequent construction of the fluid collection and disposal system (FCDS) and power plants followed.

At the end of 1995, the 110 MW_e installed capacity of Bac-Man I had generated a cumulative total of 1,151.78 GWh of electricity. This was translated to a displacement of about 1.98 million barrels of fuel oil equivalent and to approximately 32.87 million USD of foreign exchange savings based on an average price of 16.6 USD per barrel of oil (Geothermal Division DOE, 1995). The field has a total of 31 wells drilled, 21 production, 5 reinjection, and 4 exploration wells. The sum of the initial flow of some 19 wells is equivalent to 137 MW_e.

3.2 Geological framework

The Bacon-Manito geothermal system is divided into West and East Bac-Man. East Bac-Man is further subdivided into the northern Manito lowlands and the Pocdol highlands, about 10 km to the south. Within the Pocdol Highlands, eight geographical sectors are distinguished, namely: Inang Maharang (IM), Putingbato (PB), Palayangbayan (PAL), Cawayan (CW), Tanawon, Osiao, Pangas and Botong (Reyes et al., 1995).

Thermal manifestations cover an area of about 225 km^2 and consist of warm to boiling springs, solfataras, areas of copious gas emanations, and cold altered ground. Neutal Cl hot springs with temperatures of 89-96°C are in the Manito lowlands. Spring temperatures vary from 22°C to as high as 95°C. Solfataras are found in Cawayan and Pangas, with an area of copious gas emanations in Tanawon, south of Cawayan. In West Bac-Man, there are only cold to warm acid SO_4 springs and cold altered ground (Reyes et al., 1995).

The most recent volcanic events over the Pocdol highlands occurred more than 40 thousand years ago. They are related to the formation of the Tanawon and Cawayan craters, and the extrusion of the Botong and Pangas domes. Solfataric activity and areas of copious gas emanations on some of these structures also reflect their young age and probable association with the geothermal system. The youngest volcanics generally occur in regions of high subsurface temperatures, permeable formations, and active thermal manifestations (Reyes et al., 1995).

The wells in Bac-Man I intersected, from top to bottom, andesitic to basaltic lava flows and hyaloclastites, Late Miocene to Early Pliocene limestones and calcareous breccias and an intrusive complex. The latter is a sequence of cross-cutting dikes intruding the volcanic and sedimentary formations. There are about six distinct dike compositions: monzogabbro, pyroxene gabbro/diabase, hornblende and/or pyroxene microdiorite, hornblende quartz microdiorite, monzodiorite and rare aplite. Cross-cutting relationships among the dikes indicate multiple intrusive events (Reyes et al., 1995).

The major and oldest known structure that has a remarkable influence in the tectonic setting of the field is the NW-SE strike-slip fault. This major structural pattern is believed to be an extension of the Philippine Rift. Other geological structures identified in the area include volcanic centers and a collapse structure.

3.3 Production characteristics

The Bacon-Manito production field is a fracture-dominated geothermal system with reservoir temperatures in the range 260-283°C. The fractures are related to different fault trends, mainly, east, northwest and northeast, and north-northeast. The permeability is generally attributed to these faults although there are also dike intrusions and other lithologic factors to reckon with. The majority of the permeable zones is associated with well-fault intersections but lithologic contacts provide secondary permeability. Generally, the northeast trending faults are more permeable than those trending northwest.

The average porosity of the reservoir is assumed to be 8-9% while the transmissivity ranges from 2.5 to 45 mD. The initial injectivity indices of the wells as of June 1996 are within the extreme values of 9.4 and 153 l/s-MPa, respectively. During the injection tests, eight of these wells exhibited vacuum wellhead pressure. The current total mass flow of the field is measured at 900 kg/s, with about 235 kg/s of steam supplied to the power plants. The wellhead pressures during the medium-term-discharge tests vary from 0.45 to as high as 1.83 MPag, with enthalpy values ranging between 1190 and 1687 kJ/kg. At 2.5% non-condensible gases and steam rate of 2.5 kg/s-MW_e and 0.70 MPag separation pressure, the cumulative flowrate of 19 production wells corresponds to the generation of 137 MW_e of electricity.

In 1995, Bac-Man I delivered a total of 619 GWh of electricity with a utilization factor of 64.3%. The electricity generated corresponds to the utilization of 6,995 ktons of steam from 14 production wells. Five reinjection wells were capable of handling the injectivity of 665 kg/s of separated water.

4. ANALYSIS OF PRODUCTION DECLINE AND PRESSURE DRAWDOWN IN THE BAC-MAN I GEOTHERMAL PRODUCTION FIELD

Five production wells were selected for the production decline and pressure drawdown analysis using the decline curves method in Bac-Man I geothermal production field, namely, PAL-5D, PAL-7D, PAL-8D, PAL-9D and PAL-18D. The selection was made on the basis that the five wells are distributed around the reservoir boundaries of the field and that they manifest representative pressure histories of the field. The locations of the five wells are shown in Figure 1. The various pressure survey results for each well, taken at different time intervals, were plotted and pressure profiles were generated for each well, Figures 2-6.

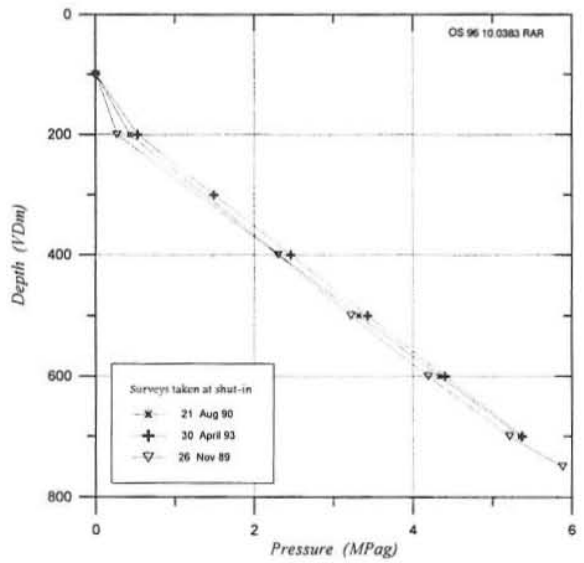

FIGURE 2: Pressure profiles for well PAL-5D

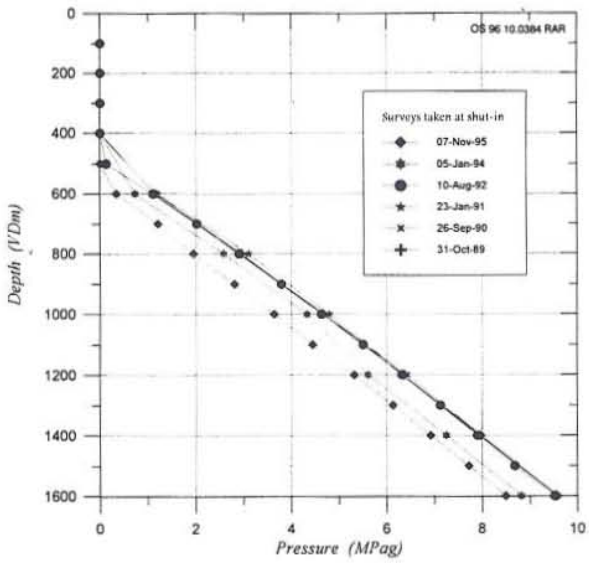

FIGURE 3: Pressure profiles for well PAL-7D

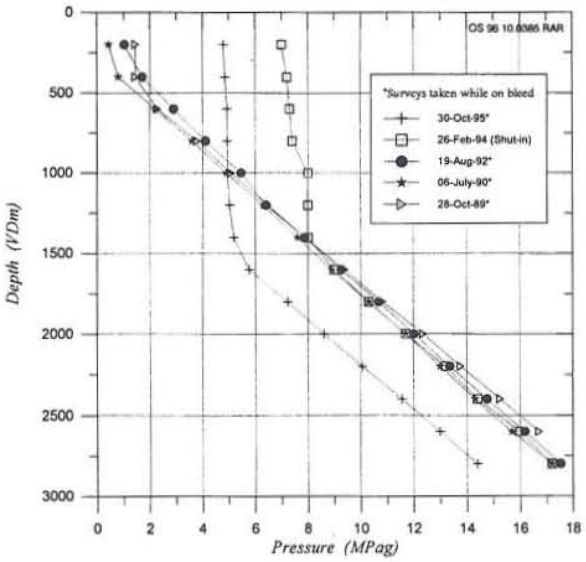

FIGURE 4: Pressure profiles for well PAL-8D

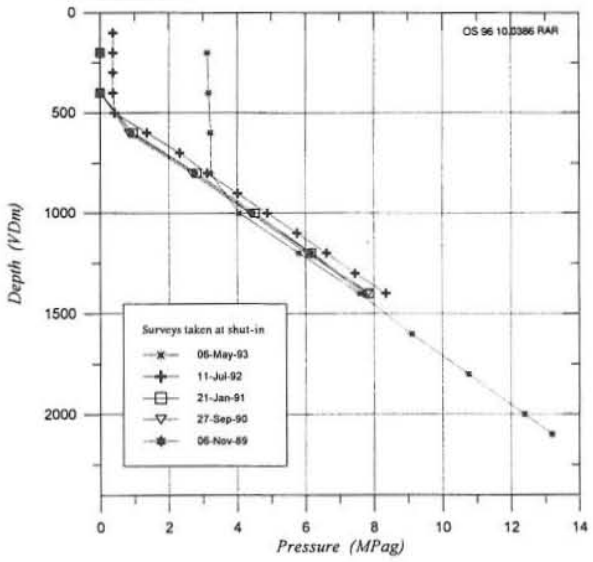

FIGURE 5: Pressure profiles for well PAL-9D

The production data (i.e. flowrate in tons/hr.) of wells PAL-8D, PAL-9D and PAL-18D for the years 1994 and 1995 were plotted against time (Figures 7-9). The total annual production of Bac-Man I field from 1993 to 1995 were also plotted against time (Figure 10).

In view of the fact that Bac-Man I geothermal field has been producing for only two years since the power plants were commissioned in late 1993, there is no considerable or crucial pressure drawdown observed in the various pressure profiles of the five production wells. Pressure drawdown demonstrated specifically by wells PAL-7D, PAL-8D and PAL-18D was not quite substantial and constructive for the decline curve analysis. For one, the downtrend in the pressure data of PAL-8D could be due to the bleeding condition under which the survey was taken and not due to depletion in the reservoir pressure. For wells PAL-8D and PAL-18D discrepancies in the calibration of the survey tools could explain the difference in the pressure taken in shut-in conditions. In order to achieve a more vivid picture and understanding of pressure drawdown in geothermal wells that relates to reservoir pressure decline, there

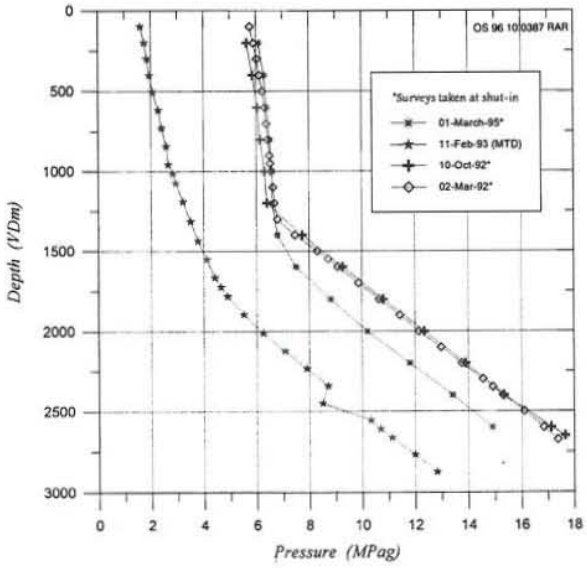

FIGURE 6: Pressure profiles for well PAL-18D

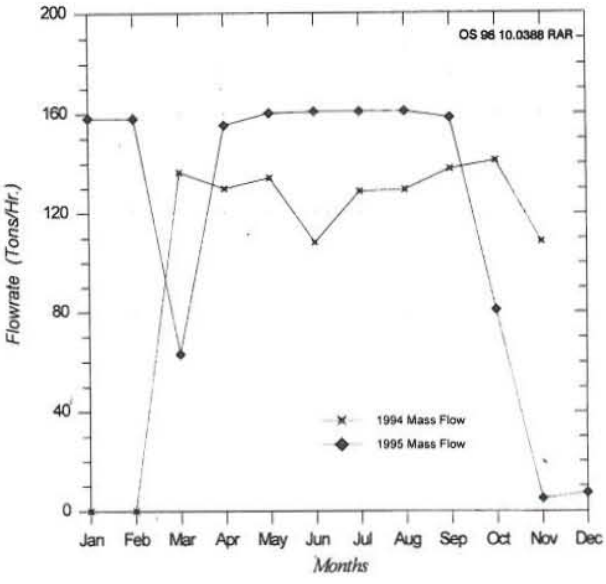

FIGURE 7: Mass flow from well PAL-8D

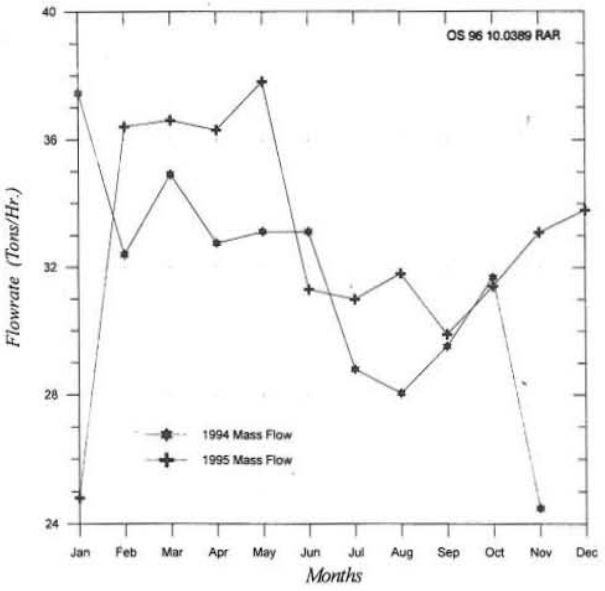

FIGURE 8: Mass flow from well PAL-9D

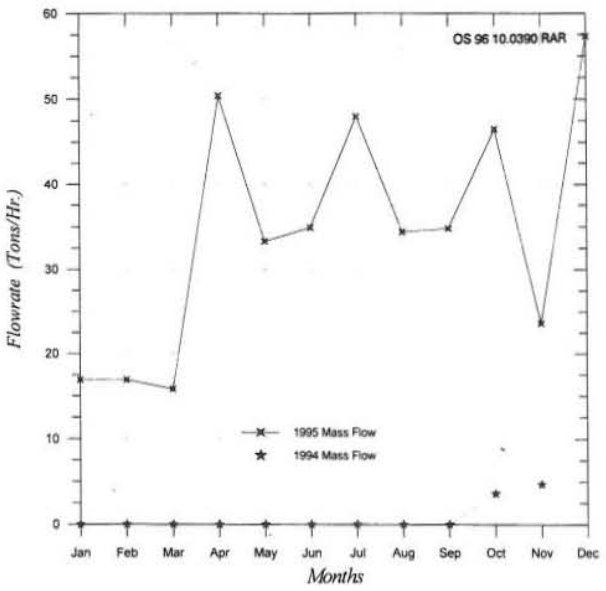

FIGURE 9: Mass flow from well PAL-18D

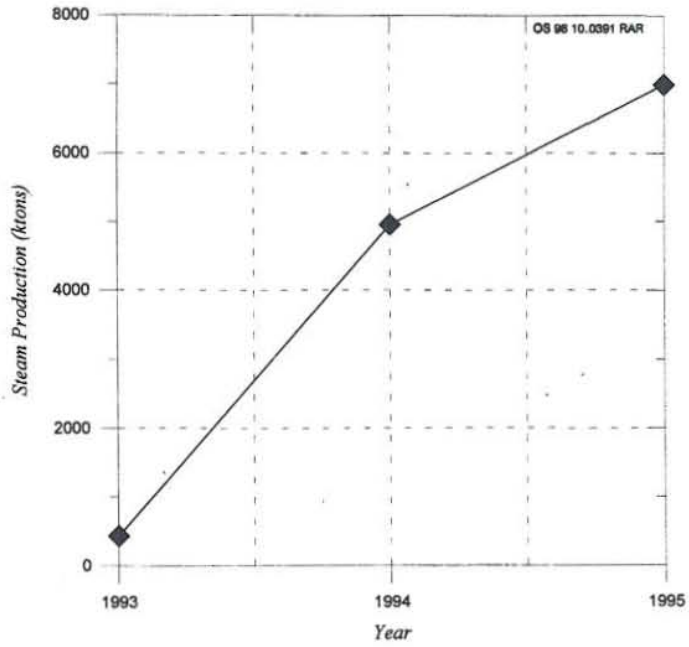

FIGURE 10: Annual steam production from the Bac-Man I production field in 1993-1995

must be other aspects taken into account. These include the flow and production histories of the wells, the time of the first production and the conditions before the surveys were taken, and the flow from the well when the pressure log was performed.

Bac-Man I has been in production only since the last quarter of 1993, and the flow and production histories of the five selected wells were not obtained. In fact, data for wells PAL-5D and PAL-7D were not available. Apparently these two wells were on standby because there was ample steam supply the last two years from Bac-Man I field. The 1994 and 1995 mass flow measurements of PAL-8D, PAL-9D and PAL-18D do not show a decline but in 1995 the three wells significantly increased their production. Incidentally, Bac-Man I field, in general, also elevated its steam production since 1993.

As a result, the objective of deducing substantial and significant pressure drawdown and production decline observations from the five representative wells which are requisites of the concocted analysis employing decline curves method was consequently defeated. No further analyses were attempted at this point in time.

4.1 Conclusions

While it is true that the major obstacle encountered in pursuing the decline curve analysis in Bac-Man I geothermal field was the unavailability at this point in time of the essential data and critical pressure

drawdown and production decline observations, it does not inevitably follow that no substantial conclusion can be drawn from the attempted analysis. If indeed there existed some depletion in the reservoir pressure of the field within the scant three years of its exploitation, then notable pressure drawdown must be very clear in the various pressure profiles of the five representative wells, considering that these wells were primarily selected for analysis because they represented illustrative pressure histories of the field. As a conclusion, the quite good behavior of Bac-Man I geothermal production field in response to exploitation may convey a notion to the Department of Energy (DOE) that though the utilization of the resource is being optimized, concomitantly proper resource management is being implemented by the developer. Currently there are no signs of over-exploitation but the DOE will steadily continue monitoring this field.

5. THE KRAFLA GEOTHERMAL FIELD

5.1 Background

The Krafla geothermal field is located in the neovolcanic zone in NE-Iceland (Figure 11), about 10 km northeast of Lake Mývatn. It is located within the Krafla caldera, which was formed about 100,000 years ago. Volcanic activity in the Krafla region is extensive and there have been several eruptive periods during the last few thousand years. The most recent one started in late 1975, with nine eruptions taking place in the Krafla volcanic system in the next decade, the last one in September 1984 (Björnsson, 1985).

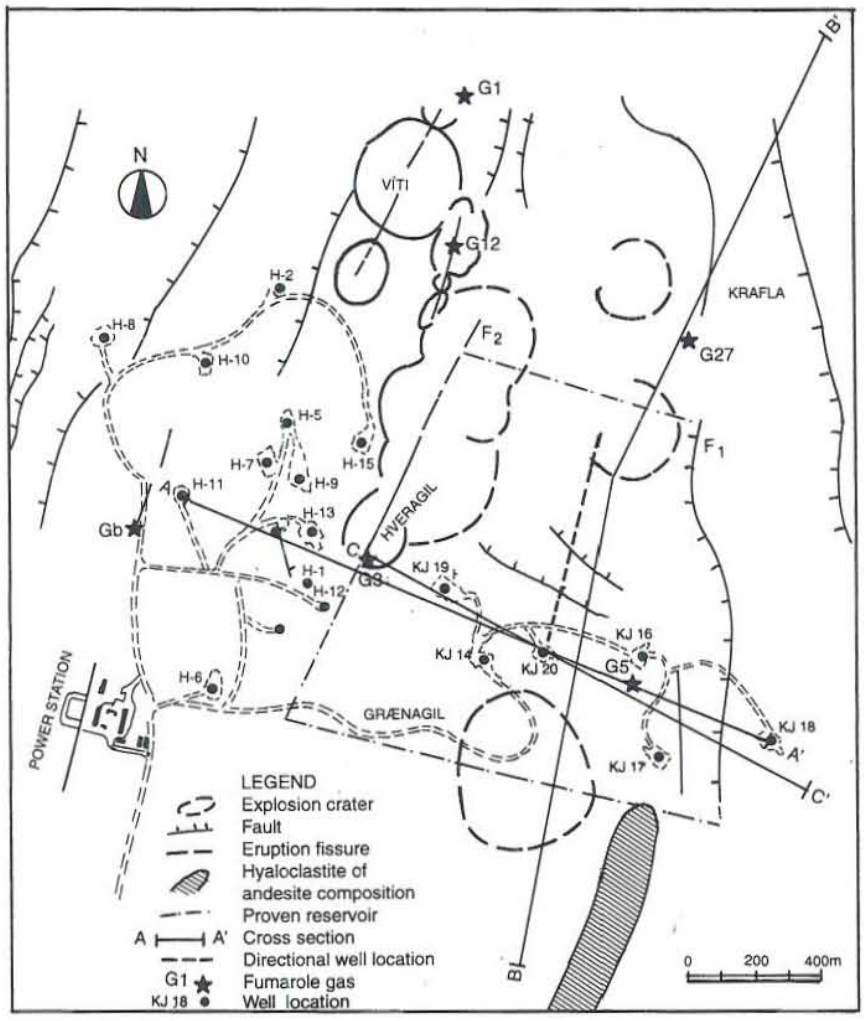

FIGURE 11: The Krafla geothermal field, wells and geological features (Ármannsson et al., 1989)

Exploration of the Krafla geothermal field started in 1970 and was initially carried out according to the Programme for the Exploration of High Temperature Areas in Iceland. A consequence of the decision to build the power plant concomitant with the drilling operation was that the investigation of the production characteristics of the field could not be made until during the production drilling phase. During drilling, it was

found that the reservoir was partly boiling and that the production characteristics were quite different from those of a water-dominated field. Up to that time all high-temperature geothermal fields in Iceland had been found to be water-dominated fields, with base temperatures of 200-300°C (Stefánsson, 1981).

The reservoir in Krafla has been found to be complicated, consisting of two geothermal zones: an upper water-dominated zone with temperatures of 205°C, and a lower zone boiling at 300-350°C. These unexpected circumstances greatly influenced the plans for the power plant. When the power plant was completed in August 1977, available steam was sufficient to produce 7 MW of electricity, whereas the power plant was designed for 60 MW_e (Stefánsson, 1981).

Currently, the 30 MW_e Krafla power station is operating at full capacity with an average annual production of about 170 GWh of electricity, with maintenance undertaken during the summer. To date, a total of 26 wells have been drilled in the Krafla high-temperature geothermal field, of which 11 production wells supply steam for the power plant.

5.2 Geological framework

The boundary between the European and the American plates runs along the axial rift zone in Iceland. In NE-Iceland it is characterized by five sub-parallel volcanic systems, which are a part of the neovolcanic zone. The Krafla volcanic center, situated northeast of Lake Mývatn is inside a 100 km long, NNE-SSW trending fissure swarm, which bisects the volcanic center in the form of a graben (Figure 11) (Ármannsson et al., 1987).

The geological features of the Mývatn region are mostly connected to the Krafla fissure swarm. The Krafla volcano features a caldera which is considered to have formed during the early part of the last interglacial period about 100,000 years ago. Since then the volcano has been very active and virtually filled the caldera with eruptive products. Acidic volcanism was initiated during its formation as is evident from an ashflow surrounding it and the rhyolite ridges in and near the eastern and western parts of the caldera rim (Jörundur, Hrafntinnuhryggur and Hlídarfjall). In the neovolcanic zone outside the caldera the basalts are mostly of olivine normative composition but predominantly quartz normative inside the caldera. The dominant geological features inside it are hyaloclastite ridges parallel to the fissure swarm and postglacial lava flows. Glacial alluvials are close to the southern rim of the caldera and large areas of the surface are covered with pyroclastics, clay and mud from explosive craters (Ármannsson et al., 1987).

The geothermal manifestations appear on the surface as mudpots and fumaroles, mostly connected to the tectonic features and faults. Hot springs are absent (Ármannsson et al., 1987).

5.3 Production characteristics

The production characteristics of the three well fields at Krafla differ widely as is apparent when simplified temperature/depth profiles for them are compared. The Leirbotnar field is divided into two distinct reservoir zones. The upper zone which extends down to approximately 1 km depth is water saturated with a mean temperature of 200-220°C. The temperature of the lower zone below 1 km depth is in excess of 300°C and boiling conditions extend below 2 km depth where the temperature is 350°C. The upper zone vanishes at the Hveragil gully and to the east of the Sudurhlídar field a boiling reservoir extends from the surface down to at least 2 km depth. In the Hvíthólar field a boiling system extends from the surface down to 700 m depth but below that the temperature drops fairly sharply to about 180°C where a deeper water saturated zone is entered, but increases again reaching about 250°C at 1900 m depth (Ármannsson et al., 1987).

Bödvarsson et al. (1984a, b, c) and Pruess et al. (1984) who developed the simulation model of the Krafla geothermal field described that the numerical model is in agreement with the assumption that the reservoir system is controlled by two upflow zones, one at Hveragil and the other close to the eastern border of the Sudurhlídar. The lower reservoir in Leirbotnar and the one in Sudurhlídar are two-phase with average vapour saturation of 10-20% (volumetric) in the fracture system. The porosity of the reservoir rock was assumed to be 5%. The permeability of the reservoir is 1-4 mD with an average of 2.0 mD. The permeability of the upflow channels at Hveragil and Sudurhlídar is estimated as 30 mD. Fluids from the upflow channel in Sudurhlídar recharge the reservoir at an estimated rate of 10 kg/s. The two phase fluid mixture flows laterally along a highly permeable fracture zone at a depth of 1 km and mixes with the upflow at Hveragil. The natural fluid flows are assumed highest at Hveragil where 8 kg/s of steam are discharged to the surface fumaroles. The remainder of the ascending fluid (13 kg/s) recharges the upper Leirbotnar reservoir (Ármannsson et al., 1987).

6. ANALYSIS OF PRODUCTION DECLINE AND PRESSURE DRAWDOWN IN THE KRAFLA GEOTHERMAL FIELD

Five production wells in the Krafla field were selected for the production and pressure decline analysis using decline curves method, namely, KJ-14, KJ-17, KJ-19, KJ-20 and KJ-21. The selection was made with the same criteria of the Bac-Man I wells, that they are distributed within the reservoir boundaries of the field and manifest representative production and pressure histories of the field (Figure 11).

The average production histories (kton/day) of the five wells for the years 1981 until 1995 were plotted against the corresponding year (Figures 12a-16a). The analysis of the type of production decline curve that each well displays was made with the program Origin version 4.0 (Microcal Software Inc., 1995).

6.1 General overview of Microcal Origin version 4.0

Microcal Origin version 4.0 is a sophisticated scientific data analysis and technical graphics software package that is designed for scientists, engineers and anyone who needs sophisticated data examination and analysis tools, surpassing flexibility in creating and controlling graphs, and superior publication-quality output. It is a complete scientific graphics system that supports a broad range of curve fitting options for linear and non-linear curves. It is a Multiple Document Interface (MDI) application and has movable, sizeable child windows. This feature allows the user to simultaneously view different visual representations of data, such as data in a worksheet versus a graph, simplifying data manipulation and analysis (Microcal Software Inc., 1995).

Linear (harmonic) curve fitting with Origin includes fitting to linear, polynomial and multiple regression equations, while nonlinear curve fitting provides common models such as exponential growth and decay, exponential associate, hyperbola, Gaussian, Lorentzian, sigmoidal and log-normal among others.

Linear functions use the linear least square regression to generate a fit curve and fitting parameters. When a type of linear regression equation is selected to start the fitting process, instantaneously the program displays the generated linear fit curve that best defines the curve in the active graph window while the fitting parameters and statistical results are recorded in the script window. Parameter initialization and fitting is carried out automatically when fitting from the linear curve fit menu. However, if the user wants to have more control over the fitting process, Origin also provides toolbars that have the curve fitting capability for polynomial and linear fits. The user can among other things specify the number of data points to be used in the fit curve dataset, specify confidence level and enable

error bars. Error bar values can be created into the active worksheet through calculating either a specified percent or the standard deviation of the dataset value and it is added to the layer of the active graph before fitting commences.

Nonlinear curve fitting with the program Origin employs the nonlinear least squares fitting to generate a fit curve in the active graph window. This nonlinear regression method is based on the Levenberg-Marquardt (LM) algorithm and is the most widely used algorithm in nonlinear least squares fitting. The simplex minimization method that can be used for parameter initialization is provided as well.

Two nonlinear least squares fitter (NLSF) modes are available, namely, basic and advanced. While both modes enable data fitting, they differ substantially in the options they provide as well as in the degree of complexity they entail. Origin's nonlinear least squares fitter starts in the basic mode. The fit curve is created by successively modifying the parameters in the selected fitting equation. This is an iterative process, in which the Origin draws a curve, checks to see how closely the curve matches the data, modifies the parameters, draws a new curve, etc., until a best fit is achieved.

However, if modification of the parameters defined in the selected function is necessitated, one can switch to the advanced mode where quite a number of modification options can be done to enable best fitting operation. The options include among others parameters initialization, parameters specification as fixed at its current value or variable during the iterative process, parameter dependancy and number of iterations. Furthermore, there are also additional fitting options provided in the advanced mode such as control fitting, parameter constraints setting, fitting output report customizing and multiple peaks fitting.

6.1.1 Chi-square (χ^2) minimization

There are two building blocks composing any fitting procedure, whether linear or nonlinear. First, the data which represent the results of some measurements in which one or several independent (input) variables were varied over a certain range in a controllable manner so as to produce the measured dependent (output) variable(s). Second is the mathematical expression (a function or a set thereof) which represents the theoretical model believed to explain the process that produced the experimental data. The model usually depends on one or more parameters.

It must be noted that the aim of the fitting procedure is to find those values of the parameters which best describe the data. The standard way of defining the best fit is to choose the parameters so that the sum of the squares (i.e. Chi-square, χ^2) of the deviations of the theoretical curve(s) from the experimental points for a range of independent variables is at its minimum. χ^2 is defined as

$$\chi^2 = \sum_{i=1}^{N} \frac{(f(x_i) - y_i)^2}{\sigma_i^2}$$

where x_i and y_i are data points, σ_i is the weight for data point i, N is the number of data points, and $f(x)$ is the fitting function. When the weights are not given, Origin displays the reduced χ^2, which is defined as

$$\chi^2 = \frac{\sum_{i=1}^{N} (f(x_i) - y_i)^2}{N - P}$$

where P is the number of parameters, and N-P is the degree of freedom. The variable χ^2 is defined as the ChiSqr variable in scripts and can be accessed as such in the program Origin.

However, there are three options for specifying the weighting method during fitting. The first one is that no weight is used for the fitting. The second option is instrumental $1/s^2$, which requires error bars to be plotted with the data where s is the error bar values. This option allows the user to specify any data column as the weights for the fit. To use this option, a weighting data column must be created and plotted as error bars. The third option is statistical $1/y$, with y as the data values. This weighting mode is suitable for data that have uncertainties proportional to the square root of the value, as in partial counts.

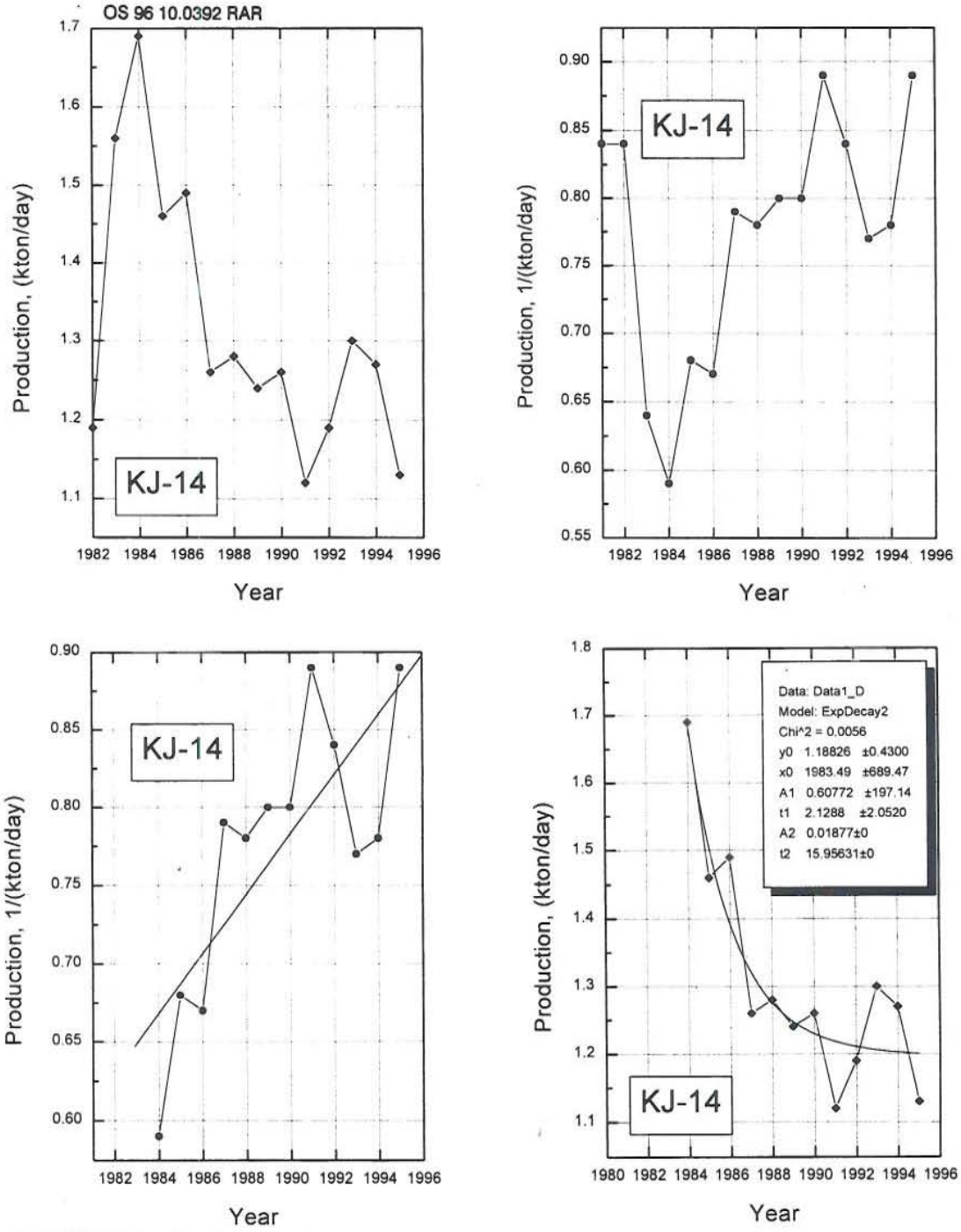

FIGURE 12: Production characteristics for well KJ-14; a) and b) Average production; c) Linear fit to the production curve; d) Non-linear fit to the production curve

6.2 Analysis of production decline curve with program Origin

6.2.1 Linear (harmonic) fitting

The datasets employed in linear (harmonic) fitting procedure were production history decline curves for the years 1981 to 1995 of wells KJ-14, KJ-17, KJ-19, KJ-20 and KJ-21. These were created by plotting the statistical data values of the average production per day of each well, 1/(kton/day), as against the corresponding year (Figures 12b-16b). The statistical $1/y$ was chosen as the weighting method that would be used in the linear fitting, hence the reciprocal of the average production values for each wells were calculated first prior to plotting versus time. As noted earlier, this weighting mode is suitable for

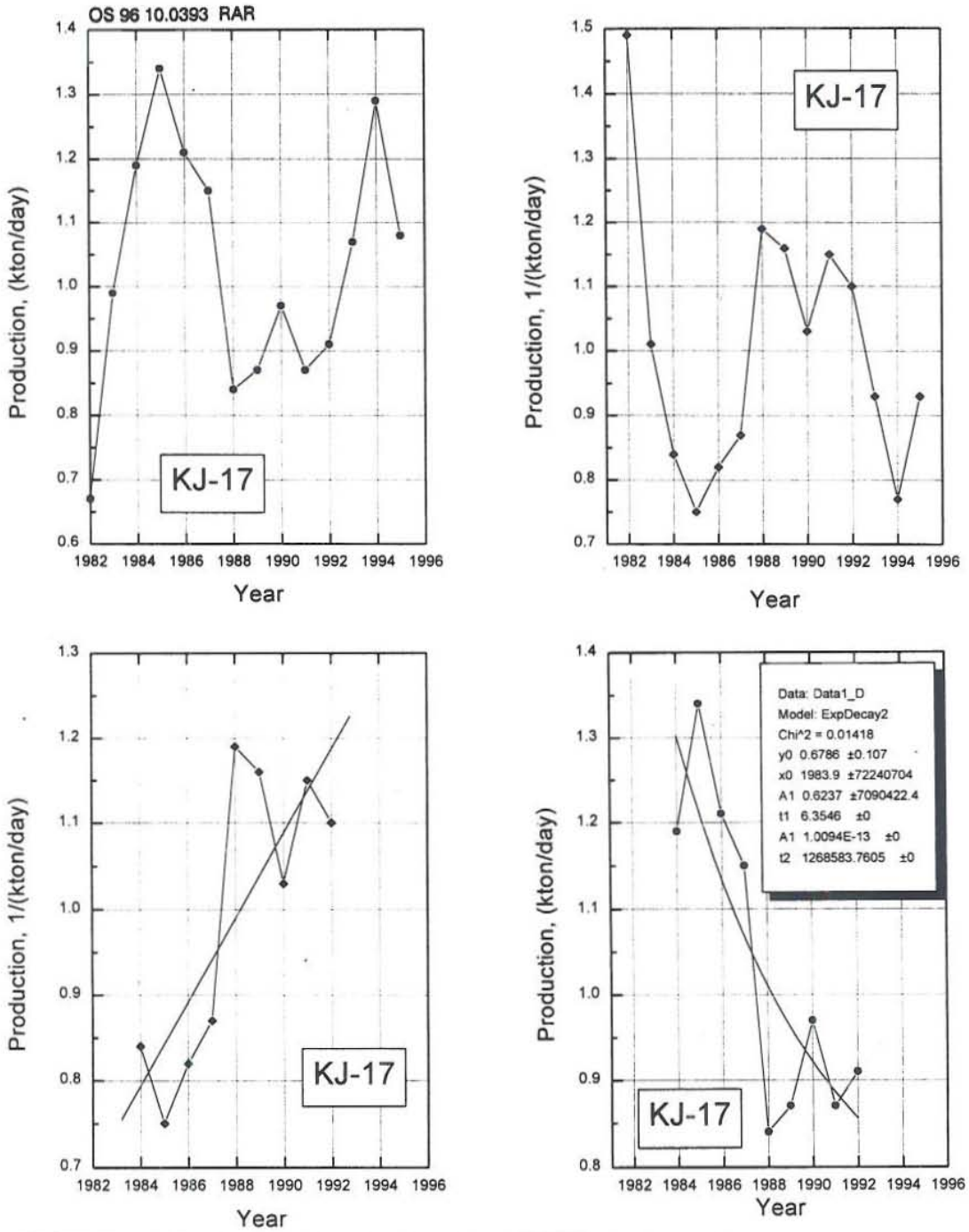

FIGURE 13: Production characteristics for well KJ-17; a) and b) Average production; c) Linear fit to the production curve; d) Non-linear fit to the production curve

data that have uncertainties proportional to the square root of the dependent y values. After fitting with the three regression equations, the best linear fit curves that define the trend of production decline foreach well were calculated using the linear regression formula

$$y = A + Bx$$

where A is the intercept value and B is the slope value. They are shown in Figures 12c-16c. After fitting, the program gives the following parameters:

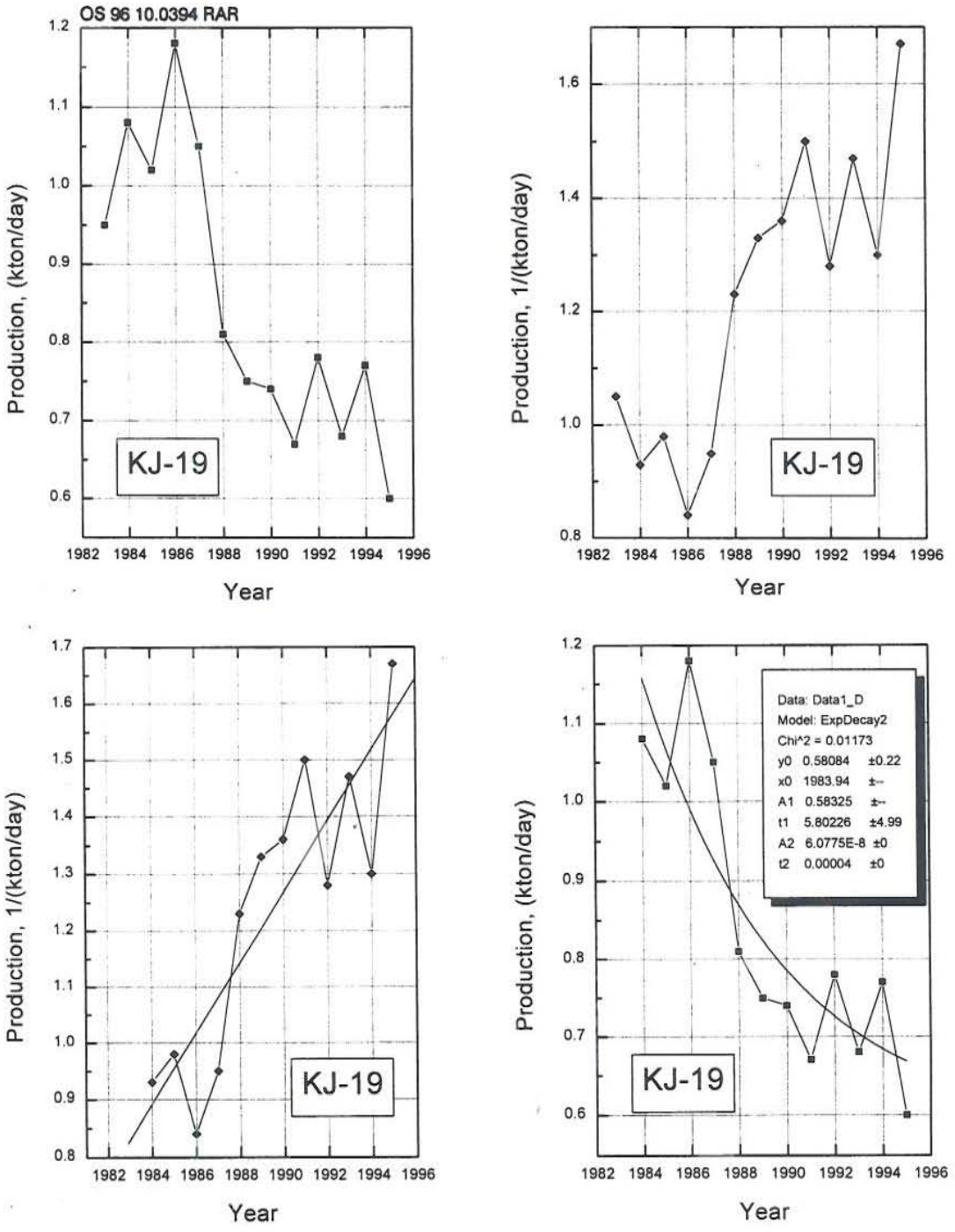

FIGURE 14: Production characteristics for well KJ-19; a) and b) Average production; c) Linear fit to the production curve; d) Non-linear fit to the production curve

A	Intercept value and standard deviation;
B	Slope value and standard deviation;
R	Correlation coefficient;
P	Probability (that R is zero);
N	Number of data points;
SD	Standard deviation of the fit, which is defined as

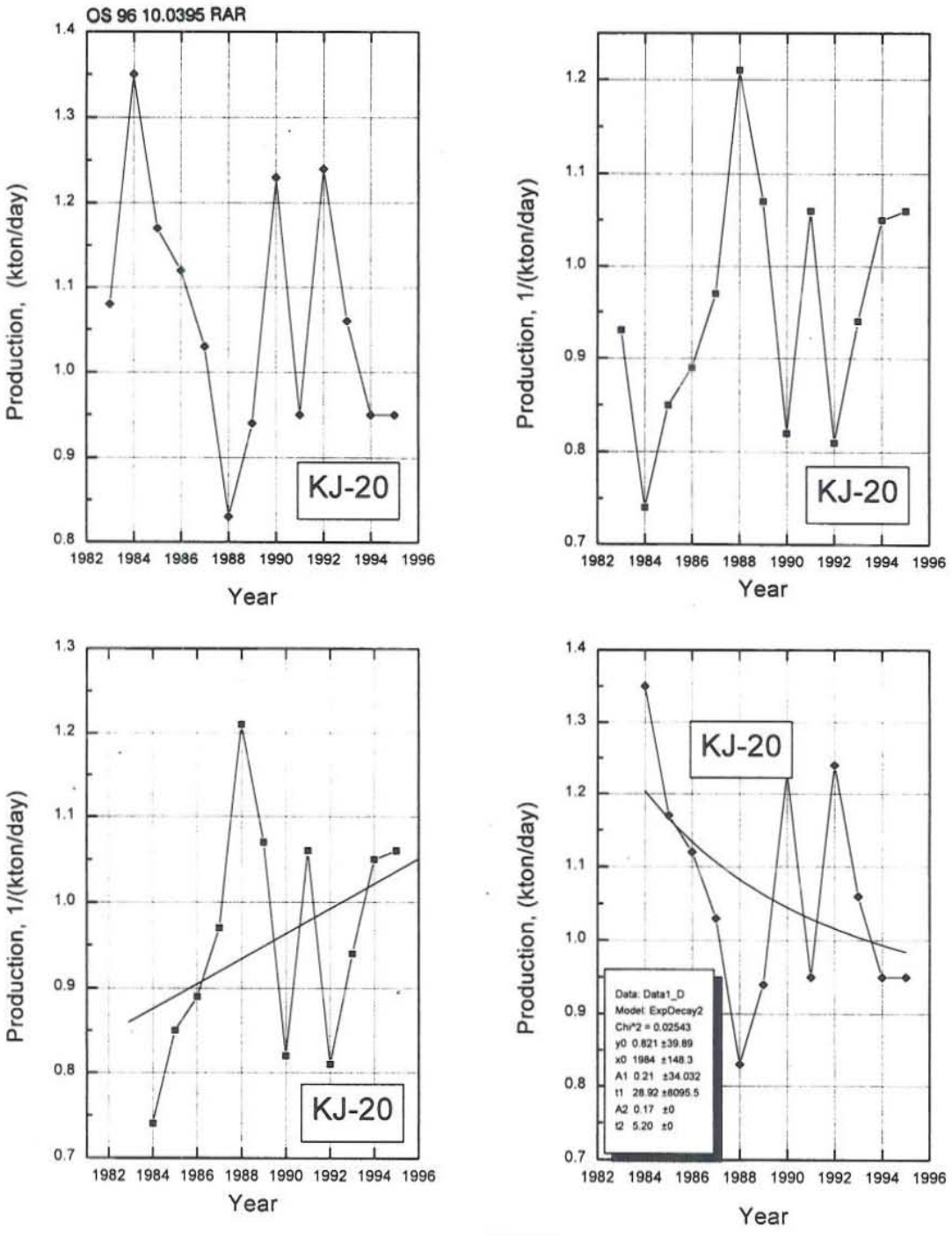

FIGURE 15: Production characteristics for well KJ-20; a) and b) Average production; c) Linear fit to the production curve; d) Non-linear fit to the production curve

$$\sqrt{\frac{\sum_{i=1}^{N}(y_i - f(x_i))^2}{N-2}}$$

where y_i are the data points, and $f(x_i)$ the fitted functional value. The Chi-square was calculated based on the following formula:

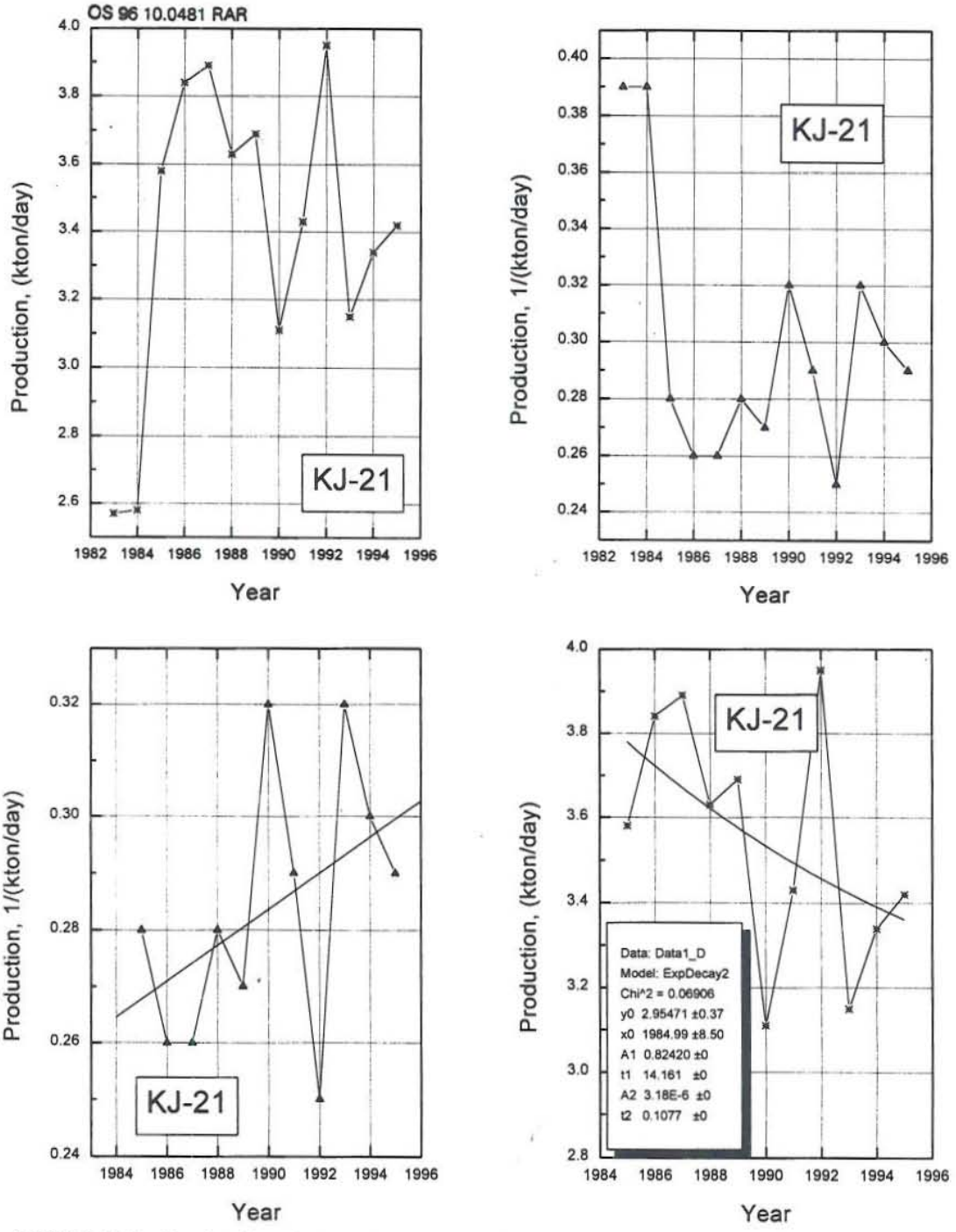

FIGURE 16: Production characteristics for well KJ-21; a) and b) Average production; c) Linear fit to the production curve; d) Non-linear fit to the production curve

$$\chi^2 = \frac{\left[\sum_{i=1}^{N} \frac{[y - f(x)]^2}{y}\right]}{(N - P)}$$

where y is the actual average production per day in a given year, i.e. 1/(kton/day), $f(x)$ is the fitted functional values, N is the number of experimental data points and P of fitted functional values. The calculated χ^2 for each linear fit curve of the five production wells are presented in Appendix I.

As shown in Figures 12c-16c, fitting with linear regression function for production wells KJ-14, KJ-17 and KJ-19 produced quite impressive linear fit curves, while the trend in production decline of wells KJ-20 and KJ-21 was poorly defined by the generated fit curves. These observations are also clearly demonstrated by the calculated χ^2 values for each production well (Table 1), whereby KJ-20 and KJ-21 have relatively higher χ^2 values as compared with the χ^2 values computed for the three remaining wells. This means that the deviation of the theoretical linear curves generated for wells KJ-20 and KJ-21 from the experimental data points used during the fitting process is greater than the amount of deviation resulting from KJ-14, KJ-17 and KJ-19 linear fitting procedures.

TABLE 1: Linear regression equation fitting parameters with the calculated Chi-square

	KJ-14	KJ-17	KJ-19	KJ-20	KJ-21
A	-37.34716	-96.75333	-123.42012	-28.05191	-6.04818
Error	9.69613	28.53951	22.28726	22.28726	4.16703
B	0.09160	0.04917	0.06266	0.01458	0.00318
Error	0.00487	0.01436	0.01120	0.01122	0.00209
R	0.77922	0.79137	0.87050	0.38003	0.45185
SD	0.05828	0.11120	0.13396	0.13420	0.02196
N	12	9	12	12	11
P	0.002810	0.01106	2.30E-04	0.22301	0.16295
χ^2	**0.030**	**0.046**	**0.035**	**0.066**	**0.056**

6.2.2 Nonlinear curve fitting

The production decline curves utilized in nonlinear curve fitting were basically the same as in linear curve fitting, only average production in a given year was not reciprocated, as shown in Figures 12d-16d. After a series of fitting procedures, it was concluded that the nonlinear curve function that best fits the trend of production decline for all five wells was the second order exponential decay using the equation

$$y = y_0 + A_1 e^{-(x-x_0)/t_1} + A_2 e^{-(x-x_0)/t_2}$$

where x_0 is the x offset, y_0 is the y offset, A is the amplitude and t is the decay constant. The resulting second order exponential decay curves that best define the production decline are shown in Figures 12d-16d. The χ^2 values for each nonlinear exponential curve were automatically calculated by the program Origin. The parameters used in the fitting process for each fit curve are shown in Table 2.

TABLE 2: Fitting parameters for exponential second order decay

Parameters	KJ-14	KJ-17	KJ-19	KJ-20	KJ-21
Y_o	1.18826	0.67859	0.58084	0.82007	2.95471
Error	0.37547	0.60503	6.9289	6.9289	0.23854
Dependancy	0.9966	0.99421	0.9998	0.9998	0.889
X_o	1983.4921	1983.9997	1983.9336	1983.9999	1984.9992
Error	108.897	146.021	163.225	7569.73	5.3377
Dependancy	0.9999	0.9999	0.9935	1	0.889
A_1	0.60772	0.62371	0.58325	0.20947	0.82422
Error	33.5528	55.0353	575.807	755.032	fixed
Dependancy	0.9999	0.9999	0.99649	1	-
t_1	2.1288	6.35463	5.80226	28.91554	14.16081
Error	1.8479	fixed	146.490	190.557	fixed
Dependancy	0.9638	-	0.9997	0.9997	-
A_2	0.01877	1.0094×10^{-13}	6.0775×10^{-8}	0.17397	3.175×10^{-6}
Error	fixed	fixed	fixed	fixed	fixed
Dependancy	-	-	-	-	-
t_2	15.95631	1268583.761	0.00004	5.20011	0.10776
Error	fixed	fixed	fixed	fixed	fixed
Dependancy	-	-	-	-	-
χ^2	**0.0056**	**0.01418**	**0.01173**	**0.02543**	**0.06906**

Figures 12d-16d illustrate that the second order exponential decay function defined prominently the production decline trend manifested by wells KJ-14, KJ-17 and KJ-19. However, the generated exponential fit curves for wells KJ-20 and KJ-21 were not quite as impressive. The calculated χ^2 values for the five wells can also strongly support this observation. From Table 2 it is clearly shown that for wells KJ-20 and more specifically KJ-21 they deviated remarkably from the other computed χ^2 values.

6.2.3 Conclusion on the type of production decline curve

The selection of which type of curve best defines and fits the production decline curves of the five Krafla wells was concluded on the basis of the χ^2 values. It must be noted that χ^2 is defined as the degree of deviation of the theoretical curve(s) from the experimental points for a range of independent variables, therefore the smaller its value the smaller the degree of deviation. The values of χ^2 resulting from both linear regression and second order exponential decay fitting functions were compared, based on the fact that the nonlinear second order exponential decay fit curves define the trend of production decline of wells KJ-14, KJ-17, KJ-19 and KJ-20 better than the linear (harmonic) fit curves, while the inverse applies for well KJ-21 (Table 3). In general though, it can be concluded that the nonlinear second order exponential decay function describes the trend in production decline observed in Krafla field.

TABLE 3: Chi-square comparison from the two fitting functions

Well no.	Sec. order expon. decay curve fit	Linear (harmonic) curve fit
KJ-14	0.006	0.030
KJ-17	0.014	0.046
KJ-19	0.012	0.035
KJ-20	0.025	0.066
KJ-21	0.069	0.056
Average	**0.0116**	**0.0466**

7. ANALYSIS OF PRESSURE DRAWDOWN AND ITS RELATIONSHIP WITH PRODUCTION DECLINE USING THE PROGRAM HOLA

7.1 General overview of the program HOLA version 3.3

HOLA (Icelandic for a well) version 3.3 is a multi-feedzone geothermal wellbore simulator written by Mr. Grímur Björnsson and Dr. Pordur Arason of Orkustofnun, Reykjavík, Iceland. The simulator produces the measured temperature and pressure profiles in flowing wells and determines the relative contribution of each feedzone for a given discharge condition. The flow within the well is assumed to be in steady-state at all times.

The simulator can handle both single and two-phase flows in vertical pipes and calculates the flowing temperature and pressure profiles in a well. It solves numerically the differential equations that describe the steady-state energy, mass and momentum flow in a vertical pipe. The code allows for multiple feedzones, variable grid spacing and radius. The code was developed in the Fortran programming language and made executable on PCs by the Microsoft 5.1 Fortran compiler (Björnsson et al., 1993).

The governing steady-state differential equations for mass, momentum and energy flux in a vertical well used by HOLA are (Björnsson et al., 1993):

$$\frac{dm}{dz} = 0 \tag{1}$$

$$\frac{dp}{dz} - [(\frac{dP}{dz})_{fri} + (\frac{dP}{dz})_{acc} + (\frac{dP}{dz})_{pot}] = 0 \tag{2}$$

$$\frac{dE_t}{dz} \pm Q = 0 \tag{3}$$

where m is the total mass flow, P is the pressure, E_t is the total energy flux in the well and z is the depth coordinate. Q denotes the ambient heat loss over a unit distance. The plus and minus signs indicate downflow and upflow, respectively. The pressure gradient is composed of three terms, wall friction, acceleration of fluid and change in gravitational load over dz.

The governing equation of flow between the well and the reservoir is (Björnsson et al., 1993):

$$m_{feed} = PI\,[\,\frac{k_{rl}\rho_l}{\mu_l} + \frac{k_{rg}\rho_g}{\mu_g}\,]\,(P_r - P_w) \tag{4}$$

where m_{feed} is the feedzone flowrate, PI is the productivity index of the feedzone, k_r is the relative permeability of the phases (subscripts l for liquid and g for steam), μ is the dynamic viscosity, ρ is density, P_r is the reservoir pressure and P_w is the pressure in the well. The relative permeabilities are calculated by linear relationships ($k_{rg} = S$ and $k_{rl} = 1\text{-}S$ where S is the volumetric steam saturation of the reservoir). Note that a flow into the well is positive and flow from the well into the formation is negative (Björnsson, 1987, Chapter 7.2).

HOLA offers six modes of calculating downhole conditions in geothermal wells (Björnsson et al., 1993):

1. *Outlet conditions known at the wellhead*: The simulator calculates pressure, temperature and saturation profiles from given wellhead conditions and given flowrates and enthalpies at each feedzone except the bottom one.

2. *Required wellhead pressure and multiple feedzones*: The simulator finds the downhole conditions that fulfill a required wellhead pressure. Also given are the productivity indices, reservoir pressure and enthalpies at each feedzone. The feedzones must have a positive flowrate.

3. *Required wellhead pressure and two feedzones*: This mode is similar to mode 2, except that only two feedzones are allowed and each can either accept or discharge fluid.

4. *Required wellhead flowrate and two feedzones*: In this mode, the simulator finds downhole conditions that fulfill a required wellhead flowrate. Only positive flow is allowed from the feedzones.
5. *Required wellhead injection rate and two feedzones*: The simulator iterates for the downhole conditions that provide the required wellhead injection rate. Only two feedzones are allowed and both must accept fluid.

6. *Variations in wellhead pressure and enthalpy for a constant flowrate and given reservoir pressure history at two feedzones*: This mode is similar to mode 4, except that now a history is specified for the reservoir pressure. Only two feedzones are allowed and both must discharge to the well.

7.2 Results of analysis with HOLA

The decline in mass flow of production wells KJ-14, KJ-17 and KJ-19 was calculated using mode 2 of program HOLA assuming the trend in the measured reservoir pressure drawdown in well KJ-18 for the years 1981, 1989 and 1992. The computed mass flow of the three wells were compared with their actual measured mass flows to find the connection of reservoir pressure drawdown observed in KJ-18 with the actual production decline observed in the three wells, and to see if this reservoir pressure depletion in KJ-18 could explain the measured decline in mass flows of the three production wells.

The analysis commenced with HOLA mode 1, whereby the bottomhole pressures and the corresponding enthalphies of the feedzones of wells KJ-14, KJ-17 and KJ-19 were calculated from given wellhead conditions and flowrates taken from actual data. The calculated bottomhole pressures with the equivalent enthalpies of feedzones were used as the initial inputs in the estimation of productivity indexes of the three wells employing HOLA mode 2 (Table 4). After series of matching and iteration processes, the calculated productivity index estimates for wells KJ-14, KJ-17 and KJ-19 are shown in Table 5.

TABLE 4: HOLA, mode 1, calculation results for the Krafla wells

Well no.	Feedzone	Depth (m)	Flow (kg/s)	Enthalpy (kJ/kg)	Bottomhole pressure (bar-a)
KJ-14	Top	0	18.00	2400.00	13.00
	1	2100	18.00	2271.84	21.16
KJ-17	Top	0	19.00	1400.00	7.00
	1	1100	19.00	1275.89	87.62
KJ-19	Top	0	16.00	1600.00	7.00
	1	1925	16.00	1399.45	23.39

TABLE 5: HOLA, mode 2, results of productivity index estimation for the Krafla wells

Well no.	Feedzone	Depth (m)	Flow (kg/s)	Enthalpy (kJ/kg)	Productivity index (m^3)	Pressure (bar-a)	Meas. reservoir pressure (bar)
KJ-14	Top	0	17.20	2056.70		12.96	
	1	2100	17.20	1930.00	0.190×10^{-11}	26.98	78
KJ-17	Top	0	19.49	1564.90		5.87	
	1	1100	19.49	1750.00	0.255×10^{-11}	62.65	90
KJ-19	Top	0	14.07	1414.64		6.96	
	1	1925	14.07	1300.00	0.520×10^{-12}	68.76	107

With the estimated productivity indexes of wells KJ-14, KJ-17 and KJ-19 and the assumed measured pressure decline in well KJ-18, the decline in mass flow of the three wells was calculated with HOLA mode 2. The results of HOLA computations are compared with the measured mass flow of the three wells (Table 6).

TABLE 6: Comparison of calculated and measured mass flow for KJ-14, KJ-17 and KJ-19

Well no.	Meas. reservoir pressure (bar)	Est. reservoir pressure (bar)	Calculated mass flow (kg/s)	Meas. mass flow (kg/s)	Year	Calc. wellhead enthalpy (kJ/kg)
KJ-14	78	75.00	14.37	15.34	1985	2580.90
		74.21	13.46	13.23	1987	2584.00
		73.00	11.82	11.73	1991	2593.40
KJ-17	90	87.00	14.90	14.06	1985	2785.00
		86.21	11.39	10.18	1990	2808.00
		85.00	9.98	9.10	1991	2809.00
KJ-19	107	104.00	9.11	10.71	1985	2641.00
		103.21	8.84	8.51	1988	2702.00
		102.00	8.63	8.11	1994	2703.80

7.3 Conclusions

Based on the results shown in Table 6, the resulting mass flows of production wells KJ-14, KJ-17 and KJ-19 calculated with the program HOLA are the same as their measured mass flow values. This means that the trend in the depletion of the reservoir pressure observed in production well KJ-18 fits the actual downtrend in production observed in the three wells and, therefore, this reservoir pressure drawdown in KJ-18 can explain the measured mass flow decline of the three wells. Further, since the second order exponential decay curve best characterizes the trend in the production decline of KJ-14, KJ-17 and KJ-19, the exponential decay function also illustrates the relationship between the reservoir pressure depletion and production decline observed in these three production wells. Future estimates of production decline of KJ-14, KJ-17 and KJ-19 can, therefore, be extrapolated assuming the trend in the reservoir pressure drawdown of KJ-18 and employing the nonlinear second order exponential decay fit function.

8. MONITORING OF GEOTHERMAL FIELDS

8.1 Parameters monitored during exploitation

There is in reality quite a number of parameters that are constantly and systematically monitored during exploitation of both high- and low-temperature geothermal fields. But for the decline curves analysis method, the parameters used are reservoir pressure and production histories and other related parameters during the flowing, shut-in and warm-up conditions of geothermal wells.

During flowing conditions of geothermal wells the variables to be recorded and monitored are mass flow, enthalpy and wellhead pressure. If the flows are dry-steam or single-phase fluid, temperature rather than enthalpy is recorded and monitored. If a downhole pump is used, pressure at or below the pump, or pumping power consumption would replace the wellhead pressure. For each well a history should be kept in a convenient form (usually a graph) that shows changes with time. Any abnormality detected should be investigated. The first step in an investigation would be to check the recent measurements made (Grant et al., 1982). Another important crucial parameter that must be measured and monitored is the drawdown in a flowing geothermal well.

At shut-in and warm-up conditions, downhole pressure and temperature profiles are measured and recorded. The determination of the pressure during warm-up period prior to well discharge is the best way to determine the initial pressure potential of a geothermal reservoir because the pressure recorded then is the undisturbed pressure of the reservoir. Soon after the start of major production, downhole pressure and temperature measurements should be made every month or every few months. Later the frequency can be decreased to once every year or two. The frequency of measurements should be adapted to the rate at which the reservoir is changing. Roughly, the measurements should be made at equal intervals of change in downhole pressure and temperature (Grant et al., 1982).

Most fields normally have some nonproductive wells that make convenient monitoring holes. When such wells are available, downhole data should be recorded more frequently, and whenever possible a continuous pressure or water level record should be obtained.

8.2 Standard operating procedures for data gathering

Proper collection of reservoir data is an unavoidable prerequisite for a meaningful analysis of reservoir conditions. The data must be as complete and clear as possible so that "bad data" can be eliminated as a possible cause of unusual results in the analysis. Some steps for ensuring good data gathering are:

1. Set up regular testing schedules and stick to them;
2. Set up calibration schedules for all instruments used such as pressure gauges and temperature tools;
3. Keep an updated calibration log for each instrument;
4. Use clear standard forms for recording data.

A data chart for routine measurements should include at least the following information:

1. Well name and location;
2. Date and time;
3. Wellhead pressure, casing, bottomhole, meter run, etc. gauge or absolute;
4. Temperature;
5. Flowrate;

6. Location of test points;
7. Units for all measured quantities;
8. Well status;
9. Type of test being conducted, i.e. buildup, interference, etc.;
10. Zone being tested;
11. Instrument numbers;
12. Name of tester.

It is recommended to keep the data in a computerized database. Such an arrangement is also of great benefit for all kinds of reservoir analyses.

8.3 Parameters detecting possible over-exploitation of geothermal reservoirs

Pressure is an essential parameter in geothermal systems. In a sense, the most important aspect in the monitoring phase of geothermal resource development and utilization can be regarded as monitoring the pressure distribution and variation in a reservoir during exploitation (Stefánsson and Steingrímsson, 1980). Pressure monitoring is indeed a process, consistently and systematically carried out to acquire information not only on the condition or performance of a single borehole, but also on the whole geothermal system as well, because it is considered the most direct approach to understanding the different physical processes occurring in the reservoir in response to exploitation.

In reality it is inevitable that depletion in the reservoir pressure of a geothermal field occurs concomitantly with exploitation of the geothermal resource. As this happens, the production output of a particular geothermal well also declines with time. It must be noted that pressure has a direct relationship with and influence on the production capacity of a particular geothermal well for it is a "property that is tied directly to the reservoir fluid." Pressure drawdown is apparently manifested by its instantenous effects on the quantitative characteristics of geothermal wells such as enthalpy, temperature, mass flow and wellhead pressure. But pressure variation with time does not only signify changes on these quantifiable parameters, it also indicates time variations in the flow pattern in the reservoir and changes in recharge or outflow.

Depletion in the reservoir pressure as a result of geothermal resource exploitation is actually the essence of pressure monitoring in the development and utilization of geothermal energy. It is the most crucial occurrence that undeniably exists during exploitation and the one that dictates the extent of geothermal field maximization and optimization. In an event that a depletion phenomenon occurs in the reservoir, or the trend in the pressure drawdown with time does not level-off as utilization of the geothermal resource is maximized and optimized, it is an instantenous signal that the geothermal field is undergoing over-exploitation. This may unmistakably change the management strategies being implemented in the geothermal field, if only to prolong the life of the geothermal resource.

While other parameters relating to both qualitative and quantitative properties of geothermal reservoirs are also constantly monitored to depict the various physical and chemical processes existing in the reservoir as exploitation proceeds, it is, however, indisputable that pressure is the most substantial reservoir parameter that would conclude existence of over-exploitation in a geothermal resource. Variations in other reservoir parameters may not seem quite alarming but existence of depletion in the reservoir pressure often triggers an immediate negative impact on the behaviour and condition of a geothermal field. Consequently, a sudden change in the resource management design would be necessitated to offset and counterbalance the depleting reservoir pressure.

9. SUMMARY AND CONCLUSIONS

In the preceding chapters, the practical application of the decline curves analysis method in depicting the type of descent in production that geothermal wells manifest was demonstrated, and the direct relationship of pressure drawdown with the production output of geothermal wells was exemplified and ascertained. Further, it was also deduced that future downtrend in production can be estimated with reservoir depletion data in one hand, and the form of decline curve function that best fits to the production decline history on the other. In the previous chapter, it was concluded that pressure is the most critical parameter that must be consistently and systematically monitored during exploitation of a geothermal resource, and the most compelling parameter that would detect possible over-exploitation of geothermal fields.

In lieu of its major mandate which is, among other things, to monitor, regulate and exercise full supervision and control over all geothermal energy projects and activities undertaken by both government and private entities to ensure proper exploitation, utilization and management of the country's geothermal resources, the employment of the decline curves analysis method can be one effective tool for the Department of Energy (DOE) in the performance of this function. The technique can enable the DOE to analyze the trend in the reservoir pressure depletion and production decline of the different production fields in the Philippines, and to estimate future decline trends. Following the results of its investigations and comparing them with the actual measurements done by the field developers, the DOE can state whether proper resource management is being implemented by the developers, or signs of over-exploitation of the resource are to be expected.

ACKNOWLEDGEMENTS

First and foremost, I would like to thank the Lord for the strength that He has bestowed on me for the past six months during the making and completion of this project.

Secondly I would like to express my gratitude to Dr. Ingvar B. Fridleifsson and Mr. Lúdvík S. Georgsson for the Fellowship award and for their ceaseless technical and moral support; Ms. Griselda J. G. Bausa and Mr. Francisco A. Benito for giving me the rare opportunity to participate in this training; Mr. Valgardur Stefánsson and Ms. Helga Tulinius for their guidance and technical assistance in making and completing this report; Mr. Grímur Björnsson and especially UNU classmate, Osvaldo Vallejos, for their patience while assisting me with the simulator HOLA; UNU lecturers and Orkustofnun employees for the doubtless genuine desires to impart their knowledge; Ms. Gudrún Bjarnadóttir for the unselfish willingness to accommodate my needs; DOE Geothermal Division staff for the endless e-mail and support and PNOC-EDC for the permission to use Bac-Man data.

Lastly, deepest thanks to my parents, my sister Rowena and her husband Allan for the care and joy they continually give my two kids, and most especially to my husband Jojo for his spiritual and moral support, and for being both a father and a mother to our two children during my six months stay in Iceland.

REFERENCES

Ármannsson, H., Benjamínsson, J., and Jeffrey, A.W.A., 1989: Gas changes in the Krafla geothermal system, Iceland. *Geochemical Geology, 76,* 175-196.

Ármannsson, H., Gudmundsson Á., and Steingrímsson, B.S., 1987: Exploration and development of the Krafla geothermal area. *Jökull, 37*, 12-29.

Björnsson, A., 1985: Dynamics of crustal rifting in NE-Iceland. *J. Geophys. Res., 90*, 151-162.

Björnsson, G., 1987: *A multi-feedzone geothermal wellbore simulator*. Lawrence Berkeley Laboratory, report LBL-23546, 8-19.

Björnsson, G., Arason, P., and Bödvarsson, G.S., 1993: *The wellbore simulator HOLA. Version 3.1. User's guide*. Orkustofnun, Reykjavík, 36 pp.

Bödvarsson, G.S., Benson, S.M., Sigurdsson, Ó., Stefánsson, V., and Elíasson, E.T., 1984a: The Krafla geothermal field, Iceland. 1. Analysis of well test data. *Water Resources Research, 20-11,* 1515-1530.

Bödvarsson, G.S., Pruess, K., Stefánsson, V., and Elíasson, E.T., 1984b: The Krafla geothermal field, Iceland. 2. The natural state of the system. *Water Resources Research, 20-11,* 1531-1544.

Bödvarsson, G.S., Pruess, K., Stefánsson, V., and Elíasson, E.T., 1984c: The Krafla geothermal field, Iceland. 3. The generating capacity of the field. *Water Resources Research, 20-11,* 1545-1559.

Geothermal Division, DOE, 1995: *1995 year-end report of the geothermal sector*. Department of Energy, Philippines, internal report, 30 pp.

Grant, M.A., Donaldson I.G., and Bixley P.F., 1982: *Geothermal reservoir engineering*. Academic Press, New York, 369 pp.

Microcal Software, Inc., 1995: *Manual on Microcal Origin: Technical graphics and data analysis in Windows*. Northampton, MA, 538 pp.

Neri, G., 1988: Production, reinjection and well testing in the Larderello geothermal field. In: Okandan, E. (editor), *Geothermal reservoir engineering*. Kluwer Academic Publishers, Dordrecht, 223-240.

Pruess, K., Bödvarsson, G.S., Stefánsson, V., and Elíasson, E.T., 1984: The Krafla geothermal field, Iceland. 4. History match and prediction of individual well performance. *Water Resources Research, 20-11,* 1561-1584.

Reyes, A.G., Zaide-Delfin, M.C., and Bueza, E.L., 1995: Petrological identification of multiple heat sources in the Bacon-Manito geothermal system, the Philippines. *Proceedings of the World Geothermal Congress 1995, Florence, Italy, 2,* 713-717.

Stefánsson, V., 1981: The Krafla geothermal field, northeast Iceland. In: Rybach, L., and Muffler, L.J.P. (editors), *Geothermal systems: Principles and case histories.* John Wiley and Son Ltd., Chichester, 273-294.

Stefánsson, V., and Steingrímsson, B.S., 1980: *Geothermal logging I: an introduction to techniques and interpretation.* Orkustofnun, Reykjavík, report OS-80017/JHD-09, 117 pp.

Zais, E.J., and Bödvarsson, G.S., 1980: *Analysis of production decline in geothermal reservoirs.* Lawrence Berkeley Laboratory, U.S., report, 75 pp.

APPENDIX I: Chi-square calculation results for the Krafla wells

KJ-14							
Year	No. of days	Cumulative production (kton)	Average product. (kton/day)	1 / production 1/(kton/day)	Calculated y 1/(kton/day)	Calculated 1/y (kton/day)	(Measured y-calc. 1/y)^2 /measured y (kton/day)
1984	245	413	1.69	0.59	0.647	1.546	0.012
1985	245	358	1.46	0.68	0.675	1.482	0.000
1986	245	366	1.49	0.67	0.703	1.422	0.003
1987	265	334	1.26	0.79	0.731	1.368	0.009
1988	280	357	1.28	0.78	0.759	1.317	0.001
1989	275	342	1.24	0.80			
1990	261	328	1.26	0.80	0.787	1.270	0.000
1991	255	285	1.12		0.815	1.226	0.011
1992	228	272	1.19	0.84			
1993	201	261	1.30	0.77	0.844	1.185	0.010
1994	215	274	1.27	0.78	0.872	1.147	0.013
1995	239	269	1.13	0.89	0.900	1.111	0.000
						Chi square:	**0.030**

KJ-17							
Year	No. of days	Cumulative production (kton)	Average product. (kton/day)	1 / production 1/(kton/day)	Calculated y 1/(kton/day)	Calculated 1/y (kton/day)	(Measured y-calc. 1/y)^2 /measured y (kton/day)
1984	245	291	1.19	0.84	0.754	1.326	0.016
1985	245	328	1.34	0.75	0.833	1.201	0.014
1986	245	297	1.21	0.82	0.911	1.097	0.011
1987	265	306	1.15	0.87			
1988	280	235	0.84	1.19	0.990	1.010	0.035
1989	275	238	0.87	1.16	1.069	0.936	0.006
1990	261	253	0.97	1.03			
1991	255	221	0.87	1.15	1.147	0.872	0.000
1992	228	208	0.91	1.10	1.226	0.816	0.010
						Chi square:	**0.046**

KJ-19							
Year	No. of days	Cumulative production (kton)	Average product. (kton/day)	1 / production 1/(kton/day)	Calculated y 1/(kton/day)	Calculated 1/y (kton/day)	(Measured y-calc. 1/y)^2 /measured y (kton/day)
1984	245	264	1.08	0.93	0.823	1.215	0.018
1985	245	250	1.02	0.98	0.915	1.093	0.005
1986	245	290	1.18	0.84	1.007	0.993	0.031
1987	265	279	1.05	0.95	1.099	0.910	0.019
1988	280	227	0.81	1.23	1.191	0.840	0.001
1989	275	207	0.75	1.33			
1990	261	192	0.74	1.36	1.283	0.780	0.003
1991	255	170	0.67	1.50	1.375	0.728	0.006
1992	228	178	0.78	1.28			
1993	201	137	0.68	1.47	1.466	0.682	0.000
1994	215	166	0.77	1.30	1.558	0.642	0.022
1995	239	143	0.60	1.67	1.650		
						Chi square:	**0.035**

KJ-20							
Year	**No. of days**	**Cumulative production (kton)**	**Average product. (kton/day)**	**1 / production 1/(kton/day)**	**Calculated y 1/(kton/day)**	**Calculated 1/y (kton/day)**	**(Measured y-calc. 1/y)^2 /measured y (kton/day)**
1984	245	330	1.35	0.74	0.860	1.163	0.025
1985	245	287	1.17	0.85	0.881	1.135	0.001
1986	245	275	1.12	0.89	0.902	1.108	0.000
1987	265	272	1.03	0.97	0.924	1.083	0.003
1988	280	232	0.83	1.21	0.945	1.058	0.064
1989	275	258	0.94	1.07			
1990	261	320	1.23	0.82	0.967	1.035	0.030
1991	255	241	0.95	1.06	0.988	1.012	0.005
1992	228	282	1.24	0.81			
1993	201	213	1.06	0.94	1.009	0.991	0.004
1994	215	204	0.95	1.05	1.031	0.970	0.000
1995	239	226	0.95	1.06	1.052	0.951	0.000
						Chi square:	**0.066**

KJ-21							
Year	**No. of days**	**Cumulative production (kton)**	**Average product. (kton/day)**	**1 / production 1/(kton/day)**	**Calculated y 1/(kton/day)**	**Calculated 1/y (kton/day)**	**(Measured y-calc. 1/y)^2 /measured y (kton/day)**
1985	245	876	3.58	0.28	0.265	3.780	0.012
1986	245	942	3.84	0.26	0.269	3.713	0.005
1987	265	1032	3.89	0.26	0.274	3.648	0.016
1988	280	1016	3.63	0.28	0.279	3.586	0.000
1989	275	1015	3.69	0.27			
1990	261	812	3.11	0.32	0.284	3.526	0.055
1991	255	875	3.43	0.29	0.288	3.467	0.000
1992	228	900	3.95	0.25			
1993	201	634	3.15	0.32	0.293	3.411	0.021
1994	215	719	3.34	0.30	0.298	3.356	0.000
1995	239	817	3.42	0.29	0.303	3.303	0.004
						Chi square:	**0.056**